Chinese Chemical Letters 35 (2024) 108652

Contents lists available at ScienceDirect

Chinese Chemical Letters

journal homepage: www.elsevier.com/locate/cclet

$ASb(SO_4)_2$ (A = Rb, Cs): Two short-wave UV antimony sulfates exhibiting large birefringence

Yang Lan[a], Jinxuan Ren[a], Pu Zhang[a], Xuehua Dong[a], Ling Huang[a,*], Liling Cao[a], Daojiang Gao[a], Guohong Zou[b,*]

[a] College of Chemistry and Materials Science, Sichuan Normal University, Chengdu 610066, China
[b] College of Chemistry, Sichuan University, Chengdu 610065, China

ARTICLE INFO

Article history:
Received 24 April 2023
Revised 16 May 2023
Accepted 5 June 2023
Available online 7 June 2023

Keywords:
Antimony sulfates
Birefringent crystals
Large birefringence
Short UV absorption edge
Stereochemically active lone pair

ABSTRACT

Herein, two antimony sulfates, named $RbSb(SO_4)_2$ (**1**) and $CsSb(SO_4)_2$ (**2**), have been successfully synthesized with the introduction of Sb^{3+} cation with stereochemically active lone pairs (SCALP) into sulfates by the conventional hydrothermal method. Both two compounds endow short ultraviolet (UV) absorption edges (281 nm and 278 nm, respectively) and large birefringence (0.171@546 nm and 0.174@546 nm, respectively), which means that they are promising short-wave UV optical materials. Interestingly, though both of the two compounds exhibit similar 1D chained structures, and possess the same functional moieties including SbO_4 seesaws and SO_4 tetrahedral groups, they exhibit significantly opposite macroscopic symmetries, *i.e.*, compound **1** crystallizes in a centrosymmetric (CS) manner ($P2_1/n$) and compound **2** in a noncentrosymmetric (NCS) manner ($P2_12_12_1$), due to the size of cations [$r(Rb^+) = 1.56$ Å, $r(Cs^+) = 1.67$ Å] affects the orientation of SCALP of the adjacent Sb^{3+}.

Short-wave ultraviolet (UV) birefringent crystals have attracted increasing interest due to their applications in the laser industry, optical communications, polarimetry, scientific instrumentations and other fields [1–10]. With the continuous development of science and technology, some birefringent crystals have been synthesized and commercialized over the last few decades, *e.g.*, $CaCO_3$ [11], YVO_4 [12], MgF_2 [13], α-BaB_2O_4 (α-BBO) [14]. However, some birefringent crystals are limited by defects such as low transmittance, small birefringence and harsh growth conditions, which severely limit their applications in the UV area. Hence, discovering new compounds with large birefringence and wide band gaps remains of great scientific and technical importance.

Based on the structure-property relationship of birefringent crystals, materials scientists have found an effective method to enhance the birefringence of optical crystals [15–18], which is to introduce the distorted metal cations contained polyhedra with stereochemically active lone pairs (SCALP) into the system, can significantly increase the probability of obtaining compounds with large birefringence. For example, a variety of high-performance Sn^{2+}/Bi^{3+}-containing birefringent materials, *e.g.*, Sn_2BO_3I (0.393@1064 nm) [19], Sn_2PO_4I (0.468@1064 nm) [19], α-SnF_2 (0.163@1064 nm) [20], $Bi(IO_3)(SO_4)$ (0.087@1064 nm) [21], $CdBi(IO_3)(SO_4)_2$ (0.1@1064 nm) [21], $KBiSO_4Cl_2$ (0.098@1064 nm) [22], have been successfully designed and synthesized by researchers. Recently, our group has conducted a series of explorations on Sb^{3+} cation, which also has an electronic configuration similar to that of the Sn^{2+}/Bi^{3+} cations, and has synthesized a number of birefringent materials with excellent properties [23], such as $CsSbF_2SO_4$ (3.0 × KDP, 0.112@1064 nm) [24], $K_2Sb(P_2O_7)F$ (4.0 × KDP, 0.157@546 nm) [25], $BaSb(H_2PO_2)_3Cl_2$ (5.0 × KDP, 0.09@546 nm) [26], $K_2Sb_2(C_2O_4)F_6$ (0.1 × KDP, 0.097@546 nm) [27]. In these compounds, the Sb^{3+} cation exhibits a variety of rich coordination patterns, *e.g.*, SbO_4F square pyramid [25], SbO_2F_2 and $SbOF_3$ seesaw [28,29], which all have large distortions that facilitate the enhancement of optical anisotropy of compounds. Also, in the total oxygen system, the Sb^{3+} cation is easy to coordinate with oxygen atoms to form asymmetric structural units, *e.g.*, SbO_3 triangular pyramid, SbO_4 seesaw, SbO_5 square pyramid and SbO_6 octahedron. By virtue of its structural diversity and flexibility, birefringent crystals with rich structures can be better obtained, and the optical properties may be improved. Recently, some total oxygen antimony-based compounds with excellent performance have been found, such as $Sb_4O_4(SO_4)(OH)_2$ (1.2 × KDP, 0.147@1064 nm) [30], $Sb_6O_7(SO_4)_2$ (2.0 × KDP, 0.052@1064 nm) [31], SbB_3O_6 (3.5 × KDP, 0.290@546 nm) [32]. Therefore, for the synthesis of optical crystals with excellent properties, the introduction of Sb^{3+} into the total oxygen system is also a good choice.

* Corresponding authors.
E-mail addresses: huangl026@sina.com (L. Huang), zough@scu.edu.cn (G. Zou).

https://doi.org/10.1016/j.cclet.2023.108652
1001-8417/

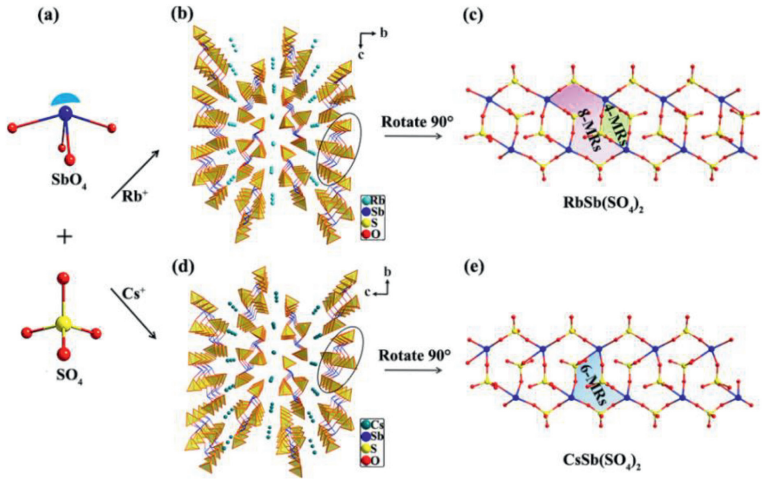

Fig. 1. (a) Ball and stick of the SbO_4 seesaw and SO_4 tetrahedron. (b, d) The 3D frame structures of compounds **1** and **2** viewed along the *bc* plane. (c) The infinite 1D $[Sb(SO_4)_2]^-_\infty$ chain for compound **1**. (e) The infinite 1D $[Sb(SO_4)_2]^-_\infty$ chain for compound **2**.

However, the introduction of metal cations containing SCALP will redshift the UV absorption edge of the compound. In order to ensure that the compound has a low UV absorption edge, the introduction of tetrahedral groups with non-π-conjugated groups (PO_4, SO_4, SeO_4) into the system is effective due to their high transmittance in the UV/deep-UV range. Plenty of high-quality phosphates and sulfates with wide transmittance bands were synthesized, *e.g.*, $LiCs_2PO_4$ (7.02 eV) [33], $RbNaMgP_2O_7$ (6.07 eV) [34], $Ba_3P_3O_{10}X$ (X = Cl, Br) (>6.22 eV) [35], $NH_4NaLi_2(SO_4)_2$ (>6.66 eV) [36], $K_2SrP_4O_{12}$ (>6.22 eV) [37], $Li_8NaRb_3(SO_4)_6{\cdot}2H_2O$ (>6.52 eV) [38].

On this basis, we have carried out a systematic study on the Sb_2O_3-A_2SO_4 (A stands for the alkali metal cations) system, and two antimony sulfates named $RbSb(SO_4)_2$ (**1**) and $CsSb(SO_4)_2$ (**2**) have been obtained by introducing Sb^{3+} cations with SCALP into sulfates. The structure of $CsSb(SO_4)_2$ has been reported by Zhao *et al.* [39]. Nevertheless, its optical properties have never been investigated. In this work, we investigated its nonlinear optical property and birefringence for the first time. Both the reported compounds exhibit wide transmission ranges (281 nm and 278 nm, respectively) and large birefringence (0.171@546 nm and 0174@546 nm, respectively). Interestingly, compounds **1** and **2** show exactly opposite macroscope symmetries due to the difference in size of the alkali metal cations. Herein, detailed characterizations and optical property measurements of the two stoichiometrically equivalent materials were performed.

The compound **1** crystallizes in the CS space group of $P2_1/n$ (No.14) and contains one independent Rb, one Sb, two S and eight O atoms in the asymmetric unit (Tables S1, S2 and S4 in Supporting information). The Sb atom forms the SbO_4 seesaw with Sb-O bond length of 2.038(11)-2.278(12) Å, and the S atom forms the SO_4 tetrahedron with S-O bond length of 1.412(14)-1.539(11) Å (Fig. 1a). In the *bc* plane, the SbO_4 seesaws and the SO_4 tetrahedra interlink by shared O atoms to form a three-dimensional (3D) framework structure. The Rb^+ cations are distributed to balance the charges in the channel extending along the *a*-axis (Fig. 1b). Each repeating unit in the 3D structure can be viewed as an infinite 1D $[Sb(SO_4)_2]^-_\infty$ chain, which contains alternating four-membered rings (4-MRs) and 8-MRs, by rotating it 90° (Fig. 1c). In this chain, each of the two SbO_4 units shares O atoms with $S2O_4$ to form a 4-MRs. Two $S1O_4$ and two $S2O_4$ form the 8-MRs basic unit by connecting with the terminal oxygen of the four SbO_4 groups.

The compound **2** crystallizes in the NCS space group of $P2_12_12_1$ (No. 19) and contains one independent Cs, one Sb, two S and eight O atoms in the asymmetric unit (Tables S1, S3, S5 in Supporting information). Similar to $RbSb(SO_4)_2$, the Sb atom adopts the SbO_4 seesaw coordination mode with Sb-O bond length of 2.043(3)-2.298(4) Å. The S atom adopts the SO_4 tetrahedron coordination mode with S-O bond length of 1.419(4)-1.544(3) Å. This compound also has a 3D frame structure similar to $RbSb(SO_4)_2$. The Cs^+ cations are distributed to balance the charges in the channel extending along the *a*-axis (Fig. 1d). Similarly, rotating the repeating unit by 90°, an infinite 1D $[Sb(SO_4)_2]^-_\infty$ chain containing 6-MRs can be observed (Fig. 1e). In this chain, three SO_4 tetrahedra form the 6-MRs basic unit by connecting with the terminal oxygen of the three SbO_4 groups. The 6-MRs units are arranged in an up-and-down staggered pattern along the *a*-axis.

From the structural descriptions of the two compounds, it is clear that the differences in the radii of the alkali metal cations cause the two examples to show different macroscopic symmetries, with compound **1** being CS while compound **2** being NCS. As shown in Fig. S1 (Supporting information), the ionic radius of Cs^+ is larger than that of Rb^+, and the greater steric hindrance causes the SbO_4 seesaw polyhedra to rotate, ultimately inducing compound **2** to crystallize in a NCS space group.

The powder X-ray diffraction (PXRD) of compounds **1** and **2** were measured. The PXRD patterns match well with the calculated data (Fig. S2 in Supporting information), indicating that the powder samples were pure phases and can be further tested.

The thermogravimetric analysis results of compounds **1** and **2** are shown in Fig. S3 (Supporting information). Compounds **1** and **2** could be stabilized up to 425 °C and 420 °C, respectively. And the decomposition products were confirmed to be Rb_2SO_4 and SbO_2, Cs_2SO_4 and SbO_2, respectively, as demonstrated by the PXRD patterns of melted samples (Fig. S4 in Supporting information).

The infrared (IR) spectra for compounds **1** and **2** are shown in Fig. S5 (Supporting information). The υ_3 (SO_4^{2-}) asymmetric stretching vibrations for compounds **1** and **2** are located at 1223, 1186, 1056, 1006 cm^{-1} and 1252, 1171, 1069, 1007 cm^{-1}, respectively. The absorption peaks of 850, 885, and 849, 887 cm^{-1} are attributed to the symmetric stretching vibration of υ_1 (SO_4^{2-}), respectively. The bands at 661, 582, 477 cm^{-1} of compound **1** belong to Sb-O asymmetric stretching and the bending. Similarly, we can observe absorption peaks for compound **2** of the Sb-O bond at

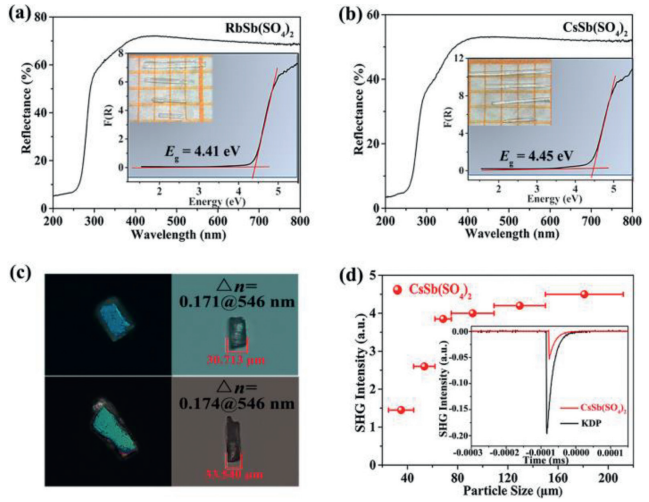

Fig. 2. (a, b) The diffuse-reflectance spectra for compounds **1** and **2** (the insert is the image of **1** and **2** crystals). (c) Birefringence measurements on the **1** and **2** crystals. (d) Phase-matching curve for compound **2**. The SHG intensity for the samples (150-212 μm) of compound **2** and KDP are shown in the insets.

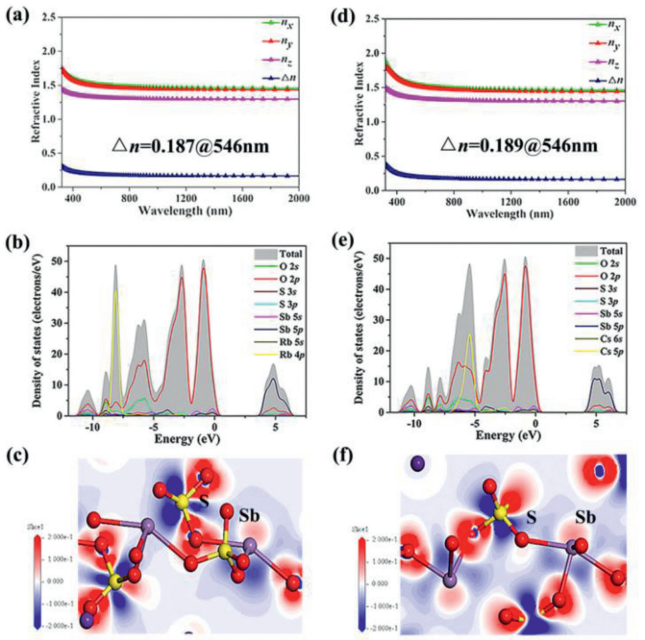

Fig. 3. Calculated refractive indices of compounds (a) **1** and (d) **2**. TDOS and PDOS of compounds (b) **1** and (e) **2**, and the E_f is normalized to 0 eV. EDD maps of compounds (c) **1** and (f) **2**.

665, 614, 578, 488 and 455 cm^{-1}. The results of the characteristic absorption peaks above are consistent with previously reported compounds [24].

The optical diffuse-reflectance spectra of compounds **1** and **2** are shown in Figs. 2a and b. The results show that their band gaps are 4.41 eV and 4.45 eV, respectively. The corresponding UV absorption edges are 281 nm and 278 nm, which indicate that both two titled compounds are potential short-wave UV optical materials.

The birefringence of compounds **1** and **2** were measured using a ZEISS Axio A1 polarizing microscope (Fig. 2c). The reported compounds exhibit the birefringence of 0.171@546 nm, 0.174@546 nm, respectively. As shown in Fig. S6 (Supporting information), we can see that the birefringence of the titled compounds are significantly larger than some other representative sulfates and phosphates, *e.g.*, $LiCs_2PO_4$ (0.008@1064 nm) [33], $NH_4NaLi_2(SO_4)_2$ (0.008@1064 nm) [36], $K_2SrP_4O_{12}$ (0.016@1064 nm) [37], $Li_8NaRb_3(SO_4)_6{\cdot}2H_2O$ (0.021@1064 nm) [38], $CsSO_3F$ (0.031@546 nm) [40], $(NH_4)_2PO_3F$ (0.035@532 nm) [41], $NaNH_4PO_3F{\cdot}H_2O$ (0.035@532 nm) [41], $Sr(NH_2SO_3)_2$ (0.056@589.3 nm) [42], $[SO_2(NH_2)_2]$ (0.07@589.3 nm) [43], $(N_2H_6)(HPO_3F)_2$ (0.077@1064 nm) [44]. And obviously, the birefringence of these two reported compounds are larger than the antimony-based sulphates/phosphates reported to date, *e.g.*, $Rb_6Sb_4(SO_4)_3F_{12}$ (0.01@1064 nm) [45], $Sb_6O_7(SO_4)_2$ (0.052@1064 nm) [31], $K_4Sb(SO_4)_3Cl$ (0.066@546 nm) [46], $NH_4SbFPO_4{\cdot}H_2O$ (0.08@1064 nm) [47], $K_2SO_4{\cdot}SbF_3$ (0.08@1064 nm) [48], $NH_4SbSO_4Cl_2$ (0.09@1064 nm) [49], $Rb_2SO_4{\cdot}SbF_3$ (0.09@1064 nm) [48], $RbSbSO_4F_2$ (0.10@1064 nm) [28], $Rb_2SO_4{\cdot}(SbF_3)_2$ (0.11@1064 nm) [50], $RbSbSO_4Cl_2$ (0.11@1064 nm) [51], $CsSbSO_4F_2$ (0.112@1064 nm) [24], $(NH_4)SbSO_4F_2$ (0.138@1064 nm) [47], $Sb_4O_4(SO_4)(OH)_2$ (0.147@1064 nm) [30], $(Gu)SbFPO_4{\cdot}H_2O$ (0.151@546 nm) [52], $K_2Sb(P_2O_7)F$ (0.157@546 nm) [25]. The calculations show that the densities of both antimony-based polyhedra and tetrahedral anions of the two reported compounds are in the middle to upper range (Table S6 in Supporting information), and the cooperative effect of the two moieties helps them to exhibit large total optical anisotropy.

For assessing the NLO coefficient of compound **2** and the powder SHG signal has been measured with 1064 nm Q-switched laser by the Kurtz-Perry method (Fig. 2d) [53]. The result indicates that the SHG efficiency is about 0.35 times that of KDP. As the particle size increases, the SHG intensity signal gradually increases, indicating that compound **2** is type-I phase matching. In order to further investigate the source of the SHG coefficient for compound **2**, dipole-moment calculations on crystallographically independent groups (SbO_4, SO_4) have been carried out (Table S7 in Supporting information). The results show that the SHG response of $CsSb(SO_4)_2$ is mainly contributed by SbO_4 groups.

To further investigate the relationship between structures and optical properties, two compounds were calculated systematically based on DFT. The calculated band gaps of compounds **1** and **2** are 3.97 and 4.35 eV, respectively, which are smaller than the experimental values, due to the GGA-PBE underestimates the band gap (Fig. S7 in Supporting information) [54].

As shown in Figs. 3a and d, the refractive index dispersion curves show that both compounds have strong anisotropy and that the birefringence values at 546 nm are 0.187 and 0.189, respectively, which are consistent with the test results.

According to the fact that compound **2** crystallizes in the $P2_12_12_1$ space group and Kleinman symmetry, it has three nonzero independent frequency doubling coefficient tensors (d_{14}, d_{25}, d_{36}). As shown in Fig. S8 (Supporting information), the absolute value of the maximum nonlinear optical coefficient d_{14} is 0.34×10^{-9} esu@1.165 eV, corresponding to $0.34 \times$ KDP, which is in agreement with the experimental value.

The partial and the total densities of states (DOS) for compounds **1** and **2** have been investigated and displayed in Figs. 3b and e. The upper regions of the valence band (VB; -10 eV to 0 eV) are mainly from O-2s, O-2p, S-3p, Rb-4p and O-2s, O-2p, S-3p, Cs-5p for compounds **1** and **2**, respectively. The conduction band (CB) bottom (0 eV to 10 eV) are both mainly attributed to the Sb-5p, O-2p, S-3p. Evidently, the electrical states in the vicinity of the forbidden band consists mainly of O-2s, O-2p, Sb-5p and S-3p orbitals, which shows that the optical characteristics of compounds **1** and **2** mainly derive from the cooperation of the SbO_4 seesaws and SO_4 tetrahedra, which can be illustrated by electron-density difference (EDD) map (Figs. 3c and f). It is clearly described that Sb^{3+} has SCALP electrons and there exists charge transfer from S to O atoms.

In summary, two alkali metal antimony sulfates, $RbSb(SO_4)_2$ (**1**) and $CsSb(SO_4)_2$ (**2**) with the same stoichiometric ratio were

successfully synthesized by the conventional hydrothermal synthesis method. The optical properties have been enhanced by introducing Sb^{3+} cations with SCALP into the sulfates, therefore the two title compounds exhibit the large birefringence (0.171 and 0.174@546 nm, respectively). Particularly, the compound **2** shows the largest birefringence value among the antimony-based sulphates/phosphates reported to date. The two title compounds endow short UV absorption edges (281 nm and 278 nm, respectively), which means that they are promising short-wave UV optical materials. Interestingly, the structural symmetries of the two compounds can be modulated by the discrepant size of alkali metal cations. This work will guide the tuning of crystal structures through metal cations and open a new door for further designing high-performance birefringent materials.

Declaration of competing interest

The authors declare that they have no known competing financial interests or personal relationships that could have appeared to influence the work reported in this paper.

Acknowledgments

The authors thank Dr. Daichuan Ma at Analytical and Testing Center, Sichuan University for technical help in the Material Studio calculations. This work was supported by the National Natural Science Foundation of China (Nos. 22122106, 22071158, 21971171), the Fundamental Research Funds from Sichuan University (No. 2021SCUNL101).

Supplementary materials

Electronic Supplementary Information (ESI) available: [additional crystallographic data, XRD patterns, IR spectra, TGA, the residue of TGA, the calculation of densities and theoretical calculation of $RbSb(SO_4)_2$ and $CsSb(SO_4)_2$. CCDC-2242196 for $RbSb(SO_4)_2$, 2242197 for $CsSb(SO_4)_2$]. Supplementary material associated with this article can be found, in the online version, at doi:10.1016/j.cclet.2023.108652.

References

[1] D. Cyranoski, Nature 457 (2009) 953–955.
[2] R.C. Youngquist, J.L. Brooks, H.J. Shaw, Opt. Lett. 8 (1983) 656–658.
[3] Y.T. Wan, Y.J. Cui, Y. Yang, et al., Chin. Chem. Lett. 32 (2021) 1511–1514.
[4] X.H. Dong, L. Huang, H.M. Zeng, et al., Angew. Chem. Int. Ed. 61 (2022) e202116790.
[5] P.S. Halasyamani, K.R. Poeppelmeier, Chem. Mater. 10 (1998) 2753–2769.
[6] Y. Zhou, Y.Q. Li, Q.R. Ding, et al., Chin. Chem. Lett. 32 (2021) 263–265.
[7] C. Wu, X.X. Jiang, Z.J. Wang, et al., Angew. Chem. Int. Ed. 60 (2021) 14806–14810.
[8] X.Y. Li, S. Semin, L.A. Estrada, et al., Chin. Chem. Lett. 29 (2018) 297–300.
[9] T.T. Tran, H.W. Yu, J.M. Rondinelli, et al., Chem. Mater. 28 (2016) 5238–5258.
[10] K.M. Ok, E.O. Chi, P.S. Halasyamani, Chem. Soc. Rev. 35 (2006) 710–717.
[11] G. Ghosh, Opt. Commun. 163 (1999) 95–102.
[12] H.T. Luo, T. Tkaczyk, E.L. Dereniak, et al., Opt. Lett. 31 (2006) 616–618.
[13] F. Sedlmeir, R. Zeltner, G. Leuchs, et al., Opt. Express 22 (2014) 30934–30942.
[14] G.Q. Zhou, J. Xu, X.D. Chen, et al., J. Cryst. Growth 191 (1998) 517–519.
[15] W.K. Wang, D.J. Mei, S.G. Wen, et al., Chin. Chem. Lett. 33 (2022) 2301–2315.
[16] G.H. Zou, L. Huang, N. Ye, et al., J. Am. Chem. Soc. 135 (2013) 18560–18566.
[17] H.W. Yu, N.Z. Koocher, J.M. Rondinelli, et al., Angew. Chem. Int. Ed. 57 (2018) 6100–6103.
[18] S.M. Liu, L. He, Y.Z. Wang, et al., Chin. Chem. Lett. 33 (2022) 1032–1036.
[19] J.Y. Guo, A. Tudi, S.J. Han, et al., Angew. Chem. Int. Ed. 60 (2021) 24901–24904.
[20] J.Y. Guo, A. Tudi, S.J. Han, et al., Angew. Chem. Int. Ed. 60 (2021) 3540–3544.
[21] Y.L. Li, C.L. Hu, J. Chen, et al., Dalton Trans. 50 (2021) 16139–16146.
[22] K.C. Chen, Y. Yang, G. Peng, et al., J. Mater. Chem. C 7 (2019) 9900–9907.
[23] G.J. Yi, G.H. Zou, Chin. J. Struct. Chem. 42 (2023) 100020.
[24] X.H. Dong, L. Huang, C.F. Hu, et al., Angew. Chem. Int. Ed. 58 (2019) 6528–6534.
[25] Y.L. Deng, L. Huang, X.H. Dong, et al., Angew. Chem. Int. Ed. 59 (2020) 21151–21156.
[26] Y. Long, X.H. Dong, L. Huang, et al., Mater. Today Phys. 28 (2022) 100876.
[27] D. Zhang, Q. Wang, T. Zheng, et al., Sci. China. Mater. 65 (2022) 3115–3124.
[28] F. Yang, L.J. Huang, X.Y. Zhao, et al., J. Mater. Chem. C 7 (2019) 8131–8138.
[29] Y.X. Chen, Z.X. Chen, Y. Zhou, et al., Chem. Eur. J. 27 (2021) 4557–4560.
[30] Q. Wei, K. Wang, C. He, et al., Inorg. Chem. 60 (2021) 11648–11654.
[31] Q. Wei, C. He, K. Wang, et al., Chem. Eur. J. 27 (2021) 5880–5884.
[32] Y.C. Liu, X.M. Liu, S. Liu, et al., Angew. Chem. Int. Ed. 59 (2020) 7793–7796.
[33] L. Li, Y. Wang, B.H. Lei, et al., J. Am. Chem. Soc. 138 (2016) 9101–9104.
[34] S.G. Zhao, X.Y. Yang, Y. Yang, et al., J. Am. Chem. Soc. 140 (2018) 1592–1595.
[35] P. Yu, L.M. Wu, L.J. Zhou, et al., J. Am. Chem. Soc. 136 (2014) 480–487.
[36] Y.Q. Li, F. Liang, S.G. Zhao, et al., J. Am. Chem. Soc. 141 (2019) 3833–3837.
[37] Z.Y. Bai, L.H. Liu, L.Z. Zhang, et al., Chem. Commun. 55 (2019) 8454–8457.
[38] Y.Q. Li, S.G. Zhao, P. Shan, et al., J. Mater. Chem. C 6 (2018) 12240–12244.
[39] X. Zhao, D.J. Mei, J.L. Xu, et al., Solid State Sci. 50 (2015) 52–57.
[40] W.Q. Jin, W.Y. Zhang, A. Tudi, et al., Adv. Sci. 8 (2021) 2003594.
[41] J. Lu, J.N. Yue, L. Xiong, et al., J. Am. Chem. Soc. 141 (2019) 8093–8097.
[42] X. Hao, M. Luo, C.S. Lin, et al., Angew. Chem. Int. Ed. 60 (2021) 7621–7625.
[43] H.T. Tian, N. Ye, M. Luo, Angew. Chem. Int. Ed. 134 (2022) e202200395.
[44] H.T. Qiu, F.M. Li, C.C. Jin, et al., Chem. Commun. 58 (2022) 5594–5597.
[45] X.H. Dong, Y. Long, X.Y. Zhao, et al., Inorg. Chem. 59 (2020) 8345–8352.
[46] F. Yang, L. Wang, Y.W. Ge, et al., J. Alloys Compd. 834 (2020) 155154.
[47] F.F. He, Y.W. Ge, X.Y. Zhao, et al., Dalton Trans. 49 (2020) 5276–5282.
[48] F.F. He, L. Wang, C.F. Hu, et al., Dalton Trans. 47 (2018) 17486–17492.
[49] F.F. He, Q. Wang, C.F. Hu, et al., Cryst. Growth Des. 18 (2018) 6239–6247.
[50] Q. Wang, L. Wang, X.Y. Zhao, et al., Inorg. Chem. Front. 6 (2019) 3125–3132.
[51] F.F. He, Y.L. Deng, X.Y. Zhao, et al., J. Mater. Chem. C 7 (2019) 5748–5754.
[52] X.H. Dong, Y. Long, L. Huang, et al., Inorg. Chem. Front. 9 (2022) 6441–6447.
[53] S.K. Kurtz, T.T. Perry, J. Appl. Phys. 39 (1968) 3798–3813.
[54] J.P. Perdew, K. Burke, M. Ernzerhof, Phys. Rev. Lett. 77 (1996) 3865–3868.